Determination of the Interdiffusion Coefficients in the Fe-Ni and Fe-Ni-P Systems below 900 °C

D. C. DEAN and J. I. GOLDSTEIN

Analytical electron microscopy was used to measure the interdiffusion coefficients, $\tilde{D}$, in the Fe-Ni and Fe-Ni-P systems between 925 and 610 °C in austenite, γ, and between 850 and 550 °C in ferrite, α. The $\tilde{D}$ values of binary γ Fe-Ni follow the extrapolated high temperature values of Goldstein *et al*. The $\tilde{D}$ values of binary α Fe-Ni are as much as two orders of magnitude lower than previously determined tracer diffusion measurements for the ferromagnetic region between 700 and 550 °C. In both ternary γ Fe-Ni-P and ternary ferromagnetic α Fe-Ni-P, the $\tilde{D}$ values are increased over the equivalent binary $\tilde{D}$ values at the same temperature. This increase is related to the ratio of the P content in the diffusion couple to the maximum P solubility in the α or γ phase at the diffusion temperature. The increase is most likely due to the effect of the electropositive solute atom P on the vacancy formation energy of the solvent, as described by LeClaire.

I. INTRODUCTION

THE Widmanstätten structure in iron meteorites, which are primarily Fe-Ni alloys, is a result of the phase transformation from single phase austenite (γ) to two phase ferrite (α) plus austenite (γ) below 900 °C in the Fe rich side of the Fe-Ni phase diagram. To model the growth of the Widmanstätten pattern in Fe-Ni, a knowledge of the volume or interdiffusion coefficient of Ni in α and γ Fe-Ni below 900 °C is required.

Reliable volume diffusion data in the Fe-Ni system are not available below 1000 °C because the volume diffusivity is very low and the effect of grain boundary diffusion is thought to predominate.[1] The recent development of analytical electron microscopy (AEM) offers the opportunity to overcome both of these problems. AEM can be used to generate quantitative chemical analysis from diffusion couples of a nanometer scale and can be used to avoid grain boundary diffusion effects.[2]

It has been observed that small additions of P (<0.3 wt pct) in Fe-Ni increase the diffusivity of Ni by up to a factor of 10 above 1000 °C in both the γ and α phases.[3] Since P ($\leqq$ 2.0 wt pct) is also present in iron meteorites and since the interdiffusion coefficients control the growth kinetics,[4] it is of interest to determine the effect of small additions of P on the diffusivity of Ni in the temperature range where the Widmanstätten pattern forms (below 900 °C). The purpose of this study is then to measure interdiffusion coefficients in austenite and ferrite in the Fe-Ni and Fe-Ni-P systems for temperatures below 900 °C with the aid of the AEM.

II. EXPERIMENTAL PROCEDURE

The Fe-Ni and Fe-Ni-P diffusion couple end member alloys were made by induction melting high purity (99.999 pct) Fe and Ni rods in a high frequency furnace under a protective argon atmosphere. The P for the ternary Fe-Ni-P alloys was provided from either of two master alloys, one of composition 10 wt pct Ni, 1 wt pct P, remainder Fe and the other of 1 wt pct P, remainder Fe. All the end member alloys were homogenized in vacuum encapsulated fused silica tubing. The binary alloys were heat treated at 1100 °C for 10 days and the ternary alloys were heat treated at 1000 °C for 10 days. The compositions of the homogeneous alloys were determined using a JEOL 733 electron probe microanalyzer (EPMA) and are given in Table I.

A 5 wt pct Ni increment was chosen between diffusion couple end members to minimize the effect of the dependence of $\tilde{D}$ on composition. Also the end member compositions for the binary α and γ couples were adjusted at each diffusion temperature in order to remain within the single phase α or γ field as seen in Figure 1. Table II lists

Table I. Diffusion Couple End Member Compositions Determined by EPMA

Binary Alloys

Designation	Desired Composition (Wt Pct)	Actual Composition (Wt Pct)
F1N	1 Ni	0.97 ± 0.01
F2N	2 Ni	2.02 ± 0.02
F5N	5 Ni	5.04 ± 0.14
F10N	10 Ni	9.95 ± 0.15
F15N	15 Ni	15.02 ± 0.04
F20N	20 Ni	19.73 ± 0.15
F25N	25 Ni	24.53 ± 0.38
F30N	30 Ni	29.57 ± 0.45

Ternary Alloys

Designation	Desired Composition (Wt Pct)	Actual Composition (Wt Pct)	
		Ni	P
FP	0.2 P	—	0.26 ± 0.05
F1Np	1 Ni, 0.2 P	0.98 ± 0.02	0.28 ± 0.05
F2NP	2 Ni, 0.2 P	1.9 ± 0.07	0.30 ± 0.05
F5NP	5 Ni, 0.2 P	4.86 ± 0.02	0.18 ± 0.02
F10NP	10 Ni, 0.2 P	9.9 ± 0.05	0.12 ± 0.01
F15NP	15 Ni, 0.2 P	14.03 ± 0.13	0.16 ± 0.03
F20NP	20 Ni, 0.2 P	19.92 ± 0.37	0.12 ± 0.04
F25NP	25 Ni, 0.2 P	24.7 ± 0.30	0.22 ± 0.03
F30NP	30 Ni, 0.2 P	29.95 ± 0.50	0.23 ± 0.05

D. C. DEAN is Metallurgist with Allegheny Ludlum, Brackenridge, PA 15014. J. I. GOLDSTEIN is Professor, Department of Metallurgy and Materials Engineering, Lehigh University, Bethlehem, PA 18015.

Manuscript submitted July 15, 1985.

the end member compositions and the diffusion temperatures and times of the α and γ diffusion couples.

The samples for the diffusion couple end members were cut with a diamond saw in parallel sections, ground, and then polished on glass plates using 1 μm diamond paste as the final step. After ultrasonic cleaning, the end members were bonded using the standard picture frame technique. The couples were then vacuum sealed inside fused silica quartz along with strips of pure tantalum which were used as oxygen getters. The quartz ampules were placed inside furnaces whose diffusion temperature was controlled to within ±3 °C. After the diffusion anneal, the couples were quenched by breaking the quartz tubes in water.

The specimen preparation technique for obtaining a thin foil diffusion couple for AEM analysis is shown schematically in Figure 2. Initially the diffusion couple was electro-spark discharge machined (EDM) with the diffusion interface parallel to the brass electrode. The resulting 3 mm diameter cylinder was glued to a metal support and cut into 4 mm wide sections. Thick cuts were necessary to avoid tearing the delicate bond interface. These sections were then ground to ~100 μm thickness with 600 grit abrasive, using ethanol as the wetting agent. After proper cleaning and drying, the specimens were electrojet polished (105 volts using a bath of 2 pct perchloric acid in ethanol, cooled to below −20 °C). The thin area resulting from the jet polish was usually not at the diffusion couple interface. The foil

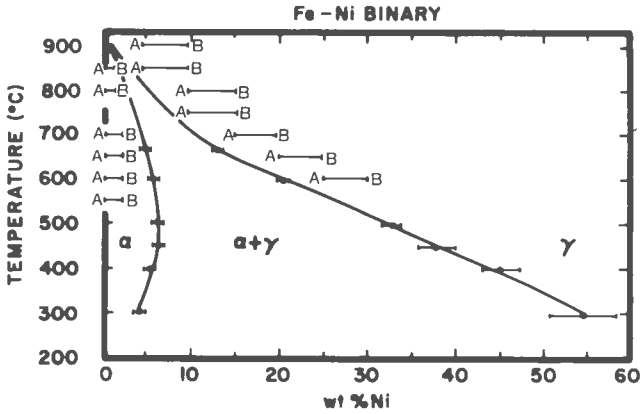

Fig. 1 — Fe-Ni phase diagram below 900 °C, as determined by Romig and Goldstein.[5] End member compositions A and B of diffusion couples in binary α and γ are shown.

Table II. Diffusion Couple Heat Treatments, Experimental Temperatures, Times, and $\tilde{D}$ Values

End Member Designations	Diffusion Temperature (°C)	Diffusion Time	$\tilde{D}$ (cm^2/sec)
		Binary Austenite	
F5N-F10N	911 ± 1	22 hours + 53 minutes	2.7×10^{-14}
F5N-F10N	851 ± 1	42 hours + 10 minutes	4.4×10^{-15}
F10N-F15N	802*	72 hours	3.6×10^{-15}*
F10N-F15N	757*	24 days	2.3×10^{-16}*
F15N-F20N	705 ± 1	40 days	1.6×10^{-16}
F20N-F25N	650 ± 2	121 days	1.2×10^{-17}
F25N-F30N	610 ± 2	62 days	4.0×10^{-18}
		Ternary Austenite Couples	
F5NP-F10NP	932 ± 1	34 hours + 50 minutes	4.7×10^{-14}
F5NP-F10NP	875 ± 1	14 hours + 35 minutes	1.7×10^{-14}
F10NP-F15NP	805	26 hours	9.6×10^{-15}
F10NP-F15NP	750*	7 days	2.0×10^{-15}*
F15NP-F20NP	705 ± 2	32 days	6.0×10^{-16}
F20NP-F25NP	650 ± 2	121 days	1.4×10^{-16}
F25NP-F30NP	610 ± 2	62 days	4.0×10^{-17}
		Binary Ferrite	
F-F1N**	853 ± 1	30 hours + 45 minutes	9.0×10^{-12}
F-F1N**	805 ± 2	31 hours	1.5×10^{-12}
F-F2N	705 ± 1	5 hours + 40 minutes	1.1×10^{-14}
F-F2N	654 ± 1	36 hours	3.3×10^{-16}
F-F2N	604 ± 1	5 days	6.8×10^{-17}
F-F2N	554 ± 3	33 days + 6 hours	1.1×10^{-17}
		Ternary Ferrite	
FP-F1NP**	844 ± 1	24 hours + 30 minutes	2.8×10^{-12}
FP-F1NP**	800 ± 1	24 hours + 30 minutes	1.7×10^{-12}
FP-F2NP	704 ± 1	6 hours + 20 minutes	6.0×10^{-14}
FP-F2NP	654 ± 3	35 hours + 45 minutes	6.0×10^{-15}
FP-F2NP	600 ± 1	6 days + 17 hours	5.5×10^{-16}
FP-F2NP	563 ± 2	31 days	1.0×10^{-15}

*Values reported by Narayan and Goldstein[2]
**Diffusion gradients measured by EPMA

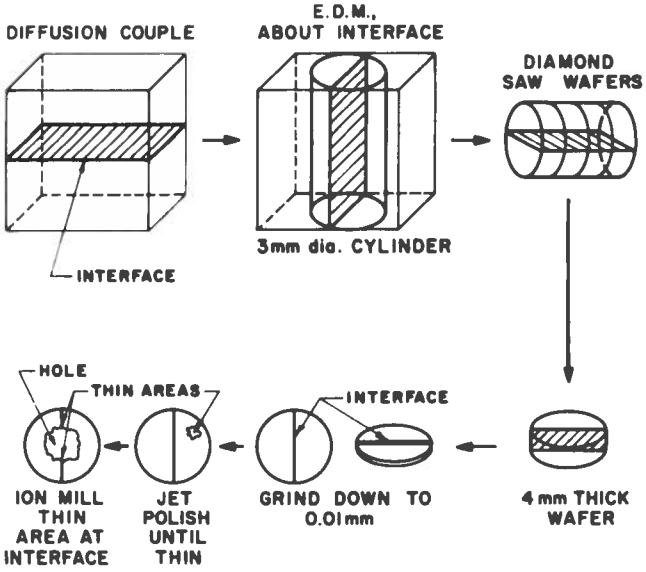

Fig. 2—Schematic of specimen preparation for AEM starting with a bonded diffusion couple. Note location of bond interface during the various stages of specimen preparation.

was then ion beam thinned until the thin area was present at the diffusion couple interface.

Chemical analysis was accomplished using a Philips EM400T AEM with an electron probe size of 20 nm for X-ray analysis. A Tracor Northern 2000 X-ray analyzer was used in conjunction with an EDAX X-ray detector, and X-ray quantification was performed with the use of the Cliff Lorimer ratio equation[6]

$$\frac{C_A}{C_B} = K_{AB}\frac{I_A}{I_B} \qquad [1]$$

where $C_{A(B)}$ = composition of element $A(B)$ in the analyzed volume
$I_{A(B)}$ = intensity of the characteristic X-ray peak of element $A(B)$
K_{AB} = proportionality or Cliff Lorimer factor. A K_{NiFe} factor of 1.21 ± 0.04 was used.[7]

The step size across the diffusion gradient varied from 50 nm to 400 nm depending on the extent of the concentration gradient. Three to four traces at different locations in the thin area were taken across the interface on each sample. The interdiffusion coefficients were determined at the Matano interface using the Boltzmann-Matano analysis.

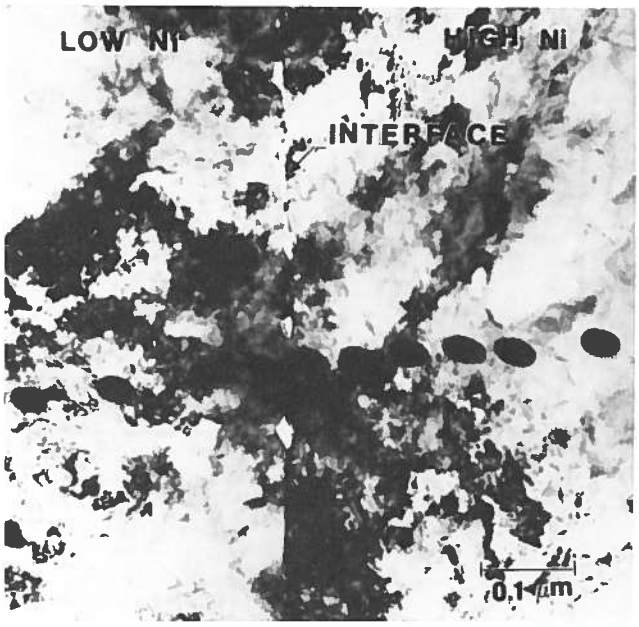

(*a*)

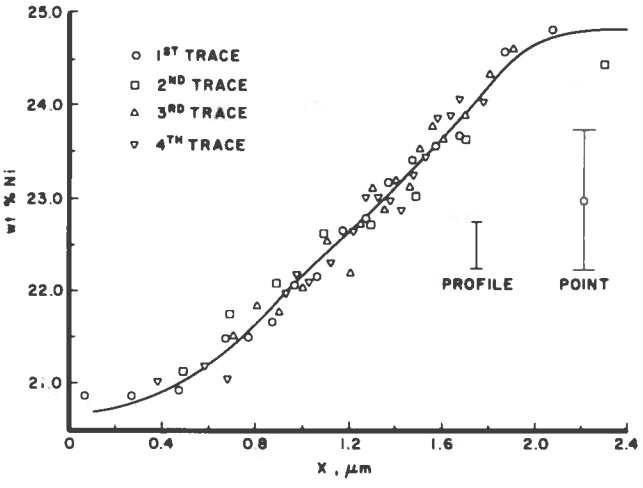

(*b*)

Fig. 3—(*a*) TEM photomicrograph of the diffusion couple bond interface in F20NP-F25NP ternary γ couple diffused at 650 °C for 121 days. Contamination spots indicating the position of the point analysis during the generation of a Ni concentration profile. The smallest step size between points was 50 nm. (*b*) Experimental Ni concentration gradient from F20NP-F25NP ternary γ couple diffused at 650 °C for 121 days. Error bars for individual points and for the best fit profile are given.

III. RESULTS AND DISCUSSION

A. *Measurement of Diffusivities*

Figure 3 shows a TEM photomicrograph of the diffusion couple bond interface and the corresponding composition profile for ternary austenite couple F20NP-F25NP diffused at 650 °C for 121 days. Figures 4(a) and 4(b) give the composition gradients for the binary austenite couple F5N-F10N diffused at 911 °C for 1 day and for the binary ferrite couple F-F2N diffused at 654 °C for 1½ days. In addition, a comparison of composition *vs* diffusion distance profiles for the ternary austenite couple, F25NP-F30NP, and the binary austenite couple, F25N-F30N, diffused in the same furnace at 610 °C for 62 days is shown in Figure 5. An order of magnitude increase in $\tilde{D}_\gamma$ is observed due to the presence of P. The values of the interdiffusion coefficients at various temperatures for the binary Fe-Ni and ternary Fe-Ni-P α and γ phases are given in Table II.

B. *Error Analysis*

The counting statistics error in the AEM data was evaluated using the following expression:[5]

$$\text{error} = \sum_{i=1}^{n} \frac{3\sqrt{N}}{N} \times 100 \pm \Delta K \qquad [2]$$

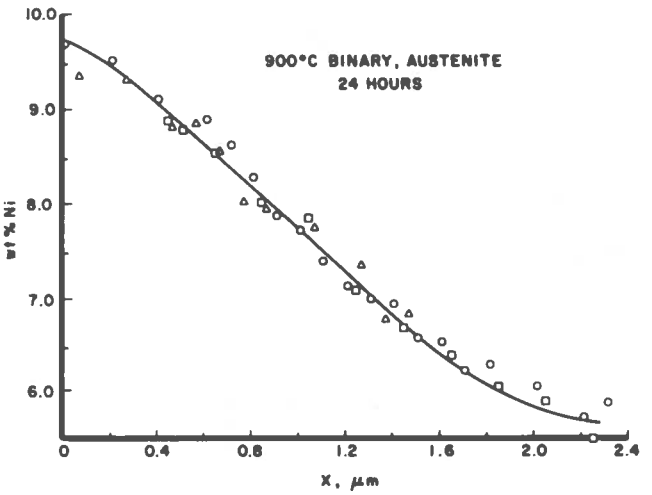

(*a*)

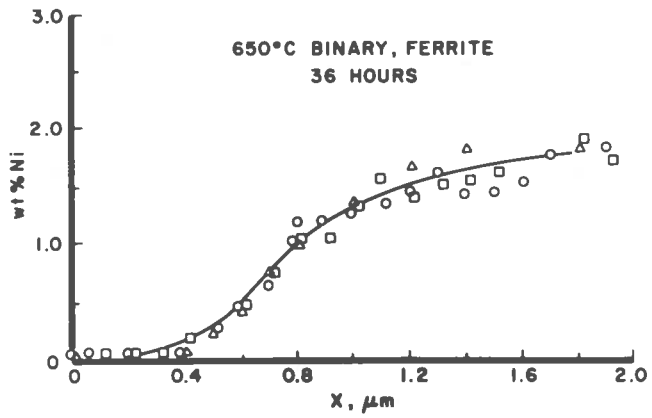

(*b*)

Fig. 4—(*a*) Experimental Ni concentration gradient for F5N-F10N binary γ couple diffused at 911 °C for 24 h. Three traces were obtained from the couple. (*b*) Experimental Ni concentration gradient for F-F2N binary α couple diffused at 654 °C for 36 h. Three traces were obtained from the couple.

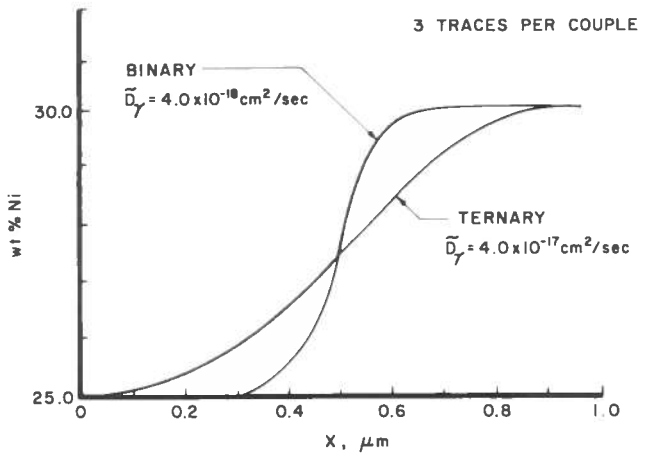

Fig. 5—Comparison between the binary and ternary γ couples F25N-F30N and F25NP-F30NP diffused together at 610 °C for 62 days. The binary diffusion distance was ~0.4 μm and the ternary diffusion distance was ~0.9 μm.

where n = number of elements i
N = number of counts in the characteristic X-ray peaks of the given element i
ΔK = error in k_{AB} proportionality or Cliff Lorimer factor determination (4 pct in the case of $k_{\text{Ni-Fe}}$).[7]

The relative error per data point from Eq. [2] was approximately ±7 pct as seen in Figure 3(b). Fortunately, the above equation overestimates the error in the present data. First, an average of four concentration gradients was generated in this sample. Therefore, N in Eq. [2] was actually four times its value at each point along the concentration gradient. Second, an internal composition calibration was present in each thin foil as the end member compositions of each couple were all previously determined by EPMA (Table I). Therefore, the error in K_{NiFe}, ΔK, can be ignored. The estimated relative error of the Ni composition data for couple F20NP-F25NP (Figure 3(b)) is reduced from ±7 pct per data point to ±2 pct. The composition data were of high enough quality that the calculated error in the Boltzmann-Matano analysis for $\tilde{D}$ was ±15 pct rel.

Binary γ couple F25N-F30N was diffused at the lowest temperature of the γ couples (610 °C) and yielded the shortest diffusion gradient (Figure 5, 400 nm) by a factor of 2.5 and the lowest diffusivity, 4.0×10^{-18} cm²/sec, by a factor of 3. A poor superposition of the composition profiles in the diffusion zone resulted since relatively little composition data were generated in the short concentration profile. A Matano analysis of this couple was not warranted due to the inaccuracy in the generated best fit profile. In order to measure the interdiffusion coefficient of couple F25N-F30N, Grube solutions were calculated for the shortest and the longest possible diffusion zones. The Grube solutions gave $\tilde{D} \cong 6 \times 10^{-18}$ cm²/sec for the longest diffusion zone and $\tilde{D} \cong 2 \times 10^{-18}$ cm²/sec for the shortest diffusion zone. The measured value was taken as 4×10^{-18} cm²/sec and the error in $\tilde{D}$ from this couple was ±50 to 100 pct.

Another source of error in the determination of $\tilde{D}$ was insufficient X-ray spatial resolution in the data points accumulated along the diffusion profile. In general, a minimum of 10 to 20 data points spaced at the limit of the X-ray spatial resolution is required for a good quality compositional analysis across the diffusion couple. In the case of the Fe-Ni(P) thin foils used in this study, the limit of the X-ray spatial resolution is ~30 to 40 nm depending on the foil thickness. Therefore, compositional gradients 500 to 1000 nm in length are necessary. Except for the F25N-F30N couple diffused at 610 °C (Figure 5), all the diffusion couples had diffusion zones 1 μm or more in length. Therefore, spatial resolution was not a source of error in the composition determination.

The F25N-F30N couple diffused at 610 °C had a diffusion zone of only 400 nm (0.4 μm) in length (Figure 5). A beam convolution program[8] was used to evaluate the effect of beam broadening on the measured concentration gradient. Only in the vicinity of the end member compositions, where a more rapid change of slope was calculated, is the beam broadening important. The deconvoluted profile did not change the measured diffusivity.

The P K_α X-rays were detected in all ternary alloys. However, the inaccuracies in X-ray counting statistics led to

an uncertainty greater than ±30 pct. Therefore, quantification of P concentration gradients, if they existed, in ternary alloys was not accomplished. Figure 6 shows that the effect of grain boundary diffusion can be identified and measured during the AEM analysis. The distortion of the concentration gradient due to grain boundary interference is clear. The effects of grain boundary diffusion were avoided in all the analyses taken with the AEM.

C. *Measurement of $\tilde{D}$ in Austenite*

1. *Binary γ*

Table III lists the known values of D_0 and Q in the formulation for $\tilde{D} = D_0 \exp(-Q/RT)$ for various Ni composition ranges in the Fe-Ni system. Figure 7 shows the variation of $\tilde{D}$ with temperature for Fe-10 wt pct Ni using the data of Table III. The variation in $\tilde{D}$ at any temperature is approximately two orders of magnitude. The effect of grain boundary diffusion, even at high temperatures, may be responsible for the spread in diffusion data. Figure 8 shows the binary interdiffusion coefficients, $\tilde{D}_\gamma$ measured in this study, as a function of temperature.

In order to correlate the extrapolated values of $\tilde{D}$ from Goldstein *et al.*[1] with the experimental values from this study, $\tilde{D}$ was calculated using the formulation given in Table III in which the value of C_{Ni} at each temperature was taken as the average Ni content in the diffusion couple. This adjustment increases C_{Ni} of the diffusion couple from 7.5 at. pct at 900 °C to 27.5 at. pct at 600 °C (Table II). Since the diffusivity of Ni increases with Ni content in Fe-Ni, the extrapolated curve of Goldstein *et al.*[1] in Figure 8 shows a nonlinear positive variation with decreasing temperature. The measured $\tilde{D}$ values follow this extrapolated curve. It is also interesting to note that Goldstein *et al.*'s diffusivity data are the lowest of the previous investigators at any temperature (Figure 7) and presumably were not affected by grain boundary diffusion.

2. *Ternary γ*

Heyward and Goldstein[3] reported a value of 1.12×10^{-13} cm²/sec for the ternary major diffusion coefficient, D^{Fe}_{NiNi}, with a P content of 0.25 wt pct at 900 °C. An extrapolated value of the $\tilde{D}_\gamma$ equal to 2.7×10^{-14} cm²/sec at 900 °C at a P content of ~0.15 wt pct was calculated from the results of this study. The value of $\tilde{D}_\gamma$ is strictly equal to D^{Fe}_{NiNi} in Fe-Ni-P only in the limit where the P concentration is zero. The difference in the values of D^{Fe}_{NiNi} and $\tilde{D}_\gamma$ at 900 °C indicates that $\tilde{D}_\gamma$ is not equal to D^{Fe}_{NiNi} even at low P concentrations (0.15 to 0.25 wt pct).

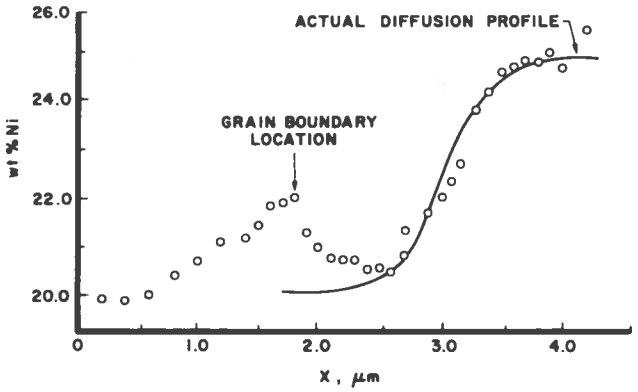

Fig. 6—Example of grain boundary diffusion compared to volume diffusion in couple F20NP-F25NP, a 650 °C ternary austenite sample diffused for 4 months. Compare actual diffusion profile to Fig. 3(b).

As shown in Figure 8, the experimental ternary diffusivity values are much larger than the binary values at low temperatures. A direct comparison of measured ternary and binary coefficients can be made at 705, 650, and 610 °C (Table II). At each of these temperatures the increase due to the effect of P is a factor of 3 or larger. It has been shown that small amounts of group Vb elements such as P, As, and Sb increase the diffusivity of the solvent in fcc binary and ternary alloys.[13,14] Hoshino *et al.*[13] demonstrated that increases in Sb from 0.3 up to 1.7 at. pct in Cu increased D^*_{Cu} up to a factor of 10. Helfmeier[14] showed that the addition of 2.7 at. pct As increased the Cu interdiffusion coefficient in CuNi by over a factor of 3. It is expected that highly electropositive solute atoms such as those of group Vb elements are strongly bound to a vacancy by the electrostatic attraction between them.[15] This effect also decreases the vacancy formation energy in the solvent and therefore raises the vacancy concentration and the resultant solvent diffusivity. Fast diffusing solutes (such as P) tend to enhance solvent diffusion rates, an effect attributable in large measure to the higher vacancy concentration.[16] Such an effect most likely explains the increased Ni diffusivity in the ternary Fe-Ni-P diffusion couples in this study.

The increase in the ratio of the experimental ternary to binary interdiffusion coefficient with temperature (Figure 8) is consistent with the fact that the solubility of P in the

Table III. Values of D_0 and Q for Chemical Volume Diffusion Coefficient in Binary Fe-Ni Austenite

Reference	Temp. Range	Wt Pct Ni Range	D_0 (cm²/sec)	Q (cal/mole)
Wells and Mehl[9]*	1450 °C to 1050 °C	4, (0.03 pct C)	0.44 ± 0.11	67,700 ± 750
		14, (0.03 pct C)	0.51 ± 0.12	67,300 ± 750
Balakir *et al.*[10]+	950 °C to 750 °C	25	0.33	60,000
Ganessan *et al.*[11]+	1100 °C to 950 °C	10	2.85×10^3	83,700
		20	2.32×10^2	76,700
Ustad and Sorum[12]+	1426 °C to 705 °C	10	0.2	63,200
		20	0.2	63,000
Goldstein *et al.*[1]+	1300 °C to 1000 °C	0 to 50	$\exp^{(0.051C_{Ni}+1.15)\dagger}$	$(76{,}400\text{-}11.6C_{Ni})^\dagger$

*chemical analysis of sectioned material
+microprobe analysis
†C_{Ni} = atomic percent Ni

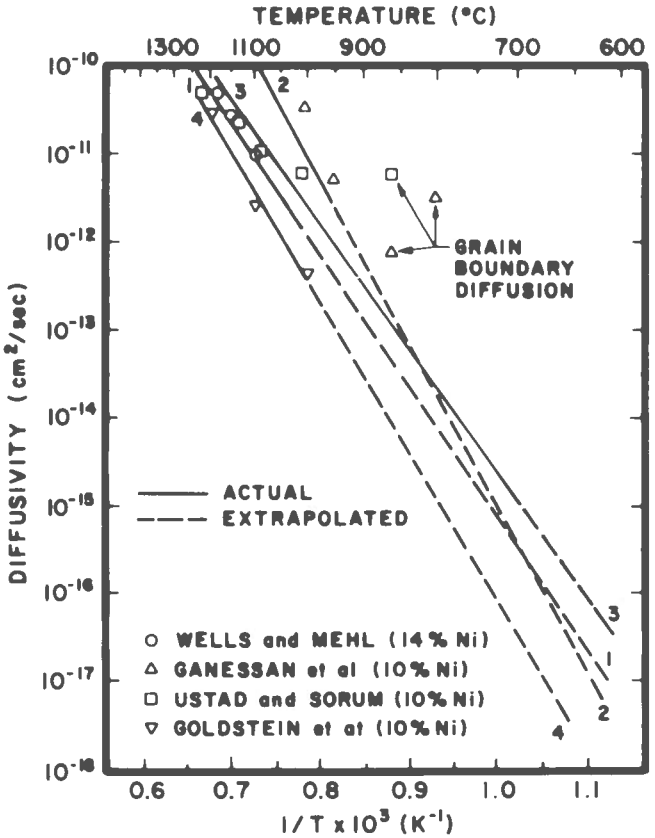

Fig. 7 — Measured and extrapolated interdiffusion coefficient values *vs* temperature for Fe-10 pct Ni. 1 — Wells and Mehl[9] measured range (1450 °C to 1050 °C); 2 — Ganessan *et al.*[11] measured range (1100 °C to 950 °C); 3 — Ustad and Sorum[12] measured range (1426 °C to 705 °C); 4 — Goldstein *et al.*[1] measured range (1300 °C to 1000 °C).

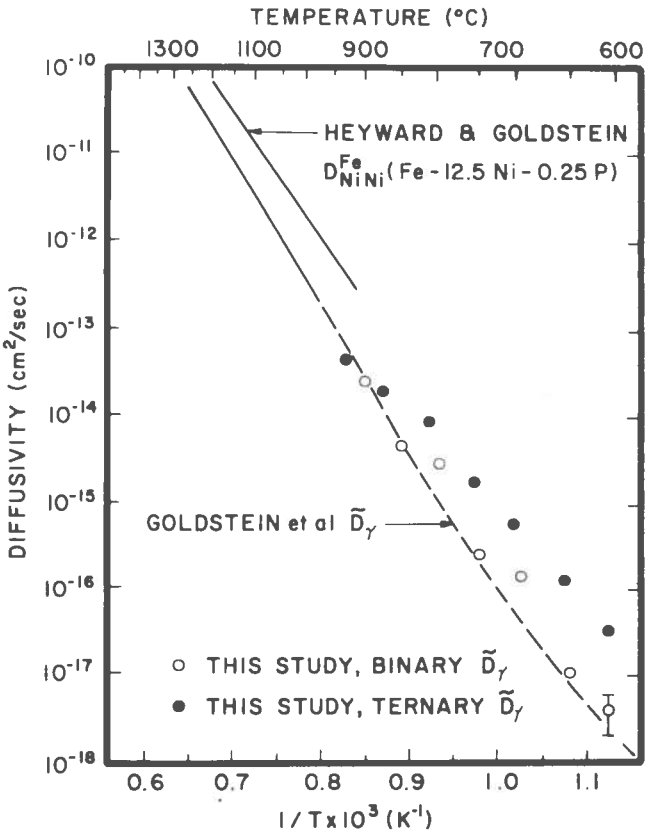

Fig. 8 — Comparison between experimental binary Fe-Ni and ternary Fe-Ni-P interdiffusion coefficients $\tilde{D}_\gamma$ in γ.

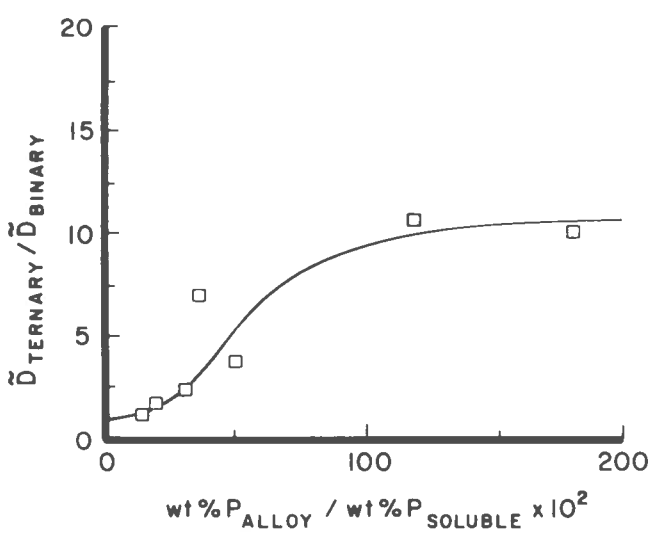

Fig. 9 — Ratios of the experimental ternary interdiffusion coefficient to the binary coefficient in γ as a function of the ratio of the average wt pct P in the ternary alloy to the wt pct P soluble in the Fe-Ni matrix at a given temperature.

diffusion couples decreases with decreasing temperature. For example, at high temperatures, 925 °C and 875 °C, the P solubility limit is above 1.0 wt pct P[17] while the P content of the diffusion couples is between 0.1 wt pct and 0.2 wt pct, far below the solubility limit of P. The corresponding increase in Ni diffusivity of the ternary couples is small (no measurable increase at 925 °C, less than two times at 875 °C). On the other hand, at 650 °C and 600 °C, where the solubility limit of P is below 0.2 wt pct P,[16] the increase in Ni diffusivity of the ternary couples is an order of magnitude. Therefore, it appears that the increase in Ni diffusivity in austenitic Fe-Ni-P depends on the ratio of the P content in the alloy to the P saturation limit in γ. Table IV lists the ratio of $\tilde{D}$ ternary to $\tilde{D}$ binary and the ratio of the P alloy content in the diffusion couple to the P solubility limit at the experimental diffusion temperatures. These data are also plotted in Figure 9. The ratio of $\tilde{D}_{\text{ternary}}$ to $\tilde{D}_{\text{binary}}$ increases from ~1.0 at P compositions far below the saturation limit (925 °C), to more than an order of magnitude increase at and above the P saturation limit (650 °C, 610 °C).

As shown by Hoshino *et al.*,[13] the increase of the solvent diffusivity by addition of a solute can be expressed by a quadratic equation given by LeClaire[16] of the form:

$$D_A^*(N_B) = D_A^*(O)\,(1 + b_1 N_B + b_2 N_B^2) \qquad [3]$$

where $D_A^*(O)$ and $D_A^*(N_B)$ are the self-diffusion coefficients of solvent A containing no B and solvent A in an alloy containing N_B atomic fraction of solute B, respectively. The terms b_1 and b_2 are constants. From an equation of this form, the maximum ratio of $D_A^*(N_B)/D_A^*(O)$ occurs at the maximum value of N_B, presumably the solubility limit of B in the solvent. If we apply Eq. [3] in its present form, we cannot solve for b_1 and b_2 since only one measured value is available at each temperature. If we simplify Eq. [3] by as-

Table IV. Ratio of the Experimental Ternary to Binary Interdiffusion Coefficient as a Function of the Ratio of the Average Phosphorus Content in the Diffusion Couple to the Phosphorus Solubility Limit at a Given Temperature in Austenite

Temperature (Approximate)	$\tilde{D}_{Ternary}/\tilde{D}_{Binary}$	Wt Pct P_{Alloy}/ Wt Pct $P_{Soluble}$
923 °C	1^+	0.15
875 °C	1.5^+	0.18
805 °C	2.5^+	0.30
750 °C	7^+	0.37
705 °C	3	0.51
650 °C	11	1.21
610 °C	10	1.83

$^+\tilde{D}_{Binary}$ is extrapolated.

suming that only the b_1 term is significant at each temperature, we get an equation of the following form:

$$D_A^*(N_B) = D_A^*(O)(1 + b_1 N_B) \quad [4]$$

Since N_B is approximately 0.2 wt pct P in each couple, we can evaluate this equation for b_1. Values of b_1 ranging from 2.5 to 50 are obtained, and these values generally increase with decreasing temperature.

D. *Measurement of $\tilde{D}$ in Ferrite*

1. *Binary α*

In binary α, above the Curie temperature of 770 °C and in the paramagnetic state, the two values of $\tilde{D}$ at 850 °C and 805 °C agree with the tracer diffusivity values (D_{Ni}^* in pure α Fe) of Borg and Lai[18] within a factor of two (Figure 10).

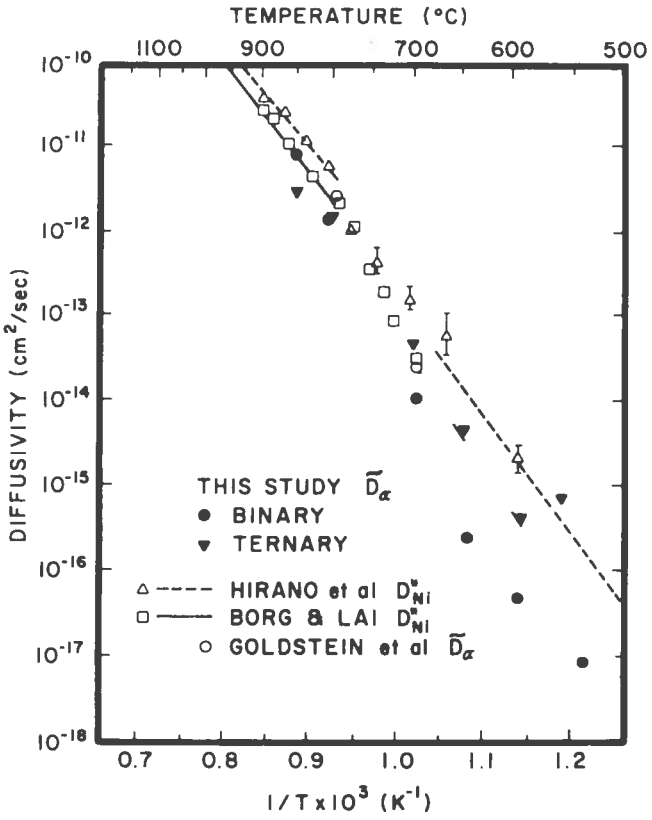

Fig. 10—Experimental binary and ternary α interdiffusion coefficients.

At the Curie temperature, approximately 770 °C, where the α Fe-Ni changes from paramagnetic state to a ferromagnetic state, Borg and Lai[18] and Hirano *et al.*[19] observed a discontinuity in the slope and value of the diffusivity of Ni. The data of this study are consistent with this discontinuity although our experimental data cannot define the discontinuity by itself.

The interdiffusion data in the ferromagnetic state, below 700 °C, are lower than the data of Hirano *et al.*[19] Unfortunately, no measurements of self diffusion were made by Borg and Lai below 700 °C. The tracer measurements made by Hirano *et al.*[19] below 700 °C are suspect due to the small thickness of the sections removed when using the residual activity method. The interdiffusion coefficient $\tilde{D}$ can be related to the self diffusion coefficients D_{Ni}^*, D_{Fe}^* by the following equation:

$$\tilde{D} = F(D_{Ni}^* N_{Fe} + D_{Fe}^* N_{Ni}) \quad [5]$$

where N_{Fe} and N_{Ni} are the atomic fractions Fe and Ni in the alloy and F is the thermodynamic factor $(1 + d \ln \gamma_{Ni}/d \ln N_{Ni})$ where γ_{Ni} is the Ni activity coefficient. The self diffusion measurements[18,19] were made in pure Fe, so that $\tilde{D} = FD_{Ni}^*$. In paramagnetic Fe, $F \cong 1$, but in ferromagnetic Fe, F is ~0.05 to 0.1. The effect of the magnetic contribution to the thermodynamics of alloys and the phase equilibria of the Fe-Ni system below ~1100 K is very significant.[20] Therefore, the four binary data points obtained in this study are now the best available interdiffusion data for the ferromagnetic α Fe-Ni phase.

2. *Ternary α*

In the paramagnetic state, at 850 °C and 800 °C, the extrapolated major diffusion coefficient D_{NiNi}^{Fe} in the α phase at 1.2 wt pct P[3] is an order of magnitude higher than the interdiffusion coefficient, $\tilde{D}$, determined in this study. As discussed for the ternary γ phase, this discrepancy in the values of D_{NiNi}^{Fe} and $\tilde{D}_\alpha$ at the same temperature indicates that $\tilde{D}_\alpha$ is not equal to D_{NiNi}^{Fe} even at low P concentrations (0.25 wt pct to 1.2 wt pct).

An apparent linearity in $\tilde{D}_\alpha$ values *vs* $1/T$ between 850 °C and 600 °C in ternary α Fe-Ni-P (Figure 10) can be observed. A discontinuity between $\tilde{D}$ values in the paramagnetic state and ferromagnetic state may exist but cannot be established directly from our data. At the higher temperatures, 844 and 800 °C, where the ratio of P content in the couple to the maximum P solubility is low, the effect of P on the diffusion of paramagnetic bcc α Fe-Ni is not significant. Bruggeman and Roberts[21] found that the self diffusion of Fe in dilute Fe-Sb increased with Sb content in the paramagnetic range. It is not clear, however, why the diffusivity of the ternary sample is lower than that of the binary sample at ~850 °C.

In the ferromagnetic state, as shown in Table V and in Figures 10 and 11, the ratio of the ternary to binary diffusivity rises as the ratio of P content in the diffusion couple to the P solubility limit increases. At 560 °C as the P content approaches the P solubility limit, the ternary interdiffusion coefficient increases dramatically, almost two orders of magnitude over the binary interdiffusion coefficient. As in the γ austenite phase, it is expected that a highly electropositive solute atom such as P will be strongly bound to a vacancy by electrostatic attraction so as to decrease the vacancy formation energy of the solvent. Such an effect

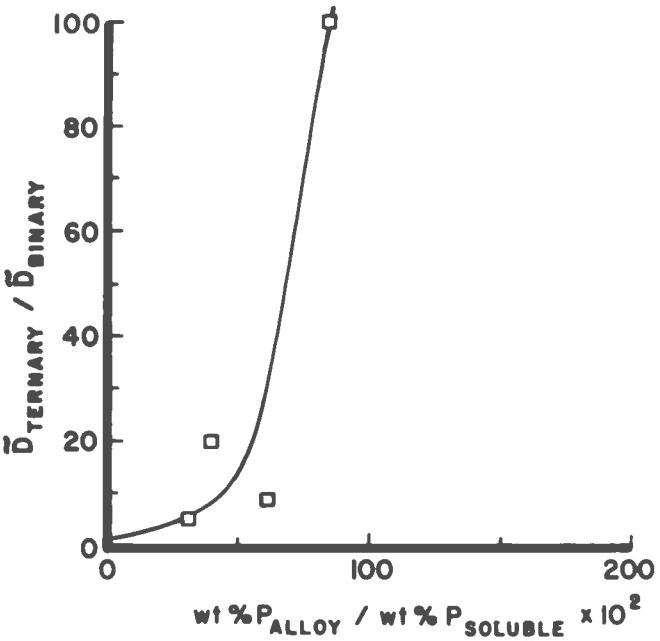

Fig. 11 — Ratio of the experimental ternary interdiffusion coefficient to the binary coefficient in α as a function of the ratio of the average wt pct P in the ternary alloy to the wt pct P soluble in the Fe-Ni matrix at a given temperature.

Table V. Ratio of the Experimental Ternary to the Extrapolated or Experimental Binary Interdiffusion Coefficient as a Function of the Ratio of the Average Phosphorus Content in the Diffusion Couple to the Phosphorus Solubility Limit at a Given Temperature in Ferrite

Temperature	$\tilde{D}_{Ternary}/\tilde{D}_{Binary}$	Wt Pct P_{Alloy}/ Wt Pct $P_{Soluble}$
705 °C	5	0.31
654 °C	18	0.41
602 °C	8	0.62
563 °C	90^+	0.82

$^+\tilde{D}_{Binary}$ is extrapolated.

probably explains the increased Ni diffusivity in ferromagnetic α iron. An increase in the self diffusion coefficient of iron of up to a factor of 2 with an addition of 0.17 wt pct P in the ferromagnetic temperature range was observed by Hänsel *et al.*[22] This increase in solvent diffusion rates is consistent with the findings of this research.

IV. SUMMARY

1. The values of $\tilde{D}$ in binary γ determined with the aid of the AEM between 910 °C and 610 °C follow the extrapolated curve from the high temperature data of Goldstein *et al.*[1]
2. The values of $\tilde{D}$ in ternary γ Fe-Ni-P show a progressive increase over the $\tilde{D}$ values in binary γ Fe-Ni from 1.0 at 932 °C to a factor of 10 below 650 °C. The increase in diffusivity is proportional to the ratio of the amount of P in the diffusion couple to the amount of P soluble in γ at the diffusion temperature. The effect of P is explained by the strong electrostatic attraction between group Vb elements and vacancies in the FeNi solvent.
3. In binary paramagnetic α Fe-Ni, the values of $\tilde{D}$ determined by EPMA at 853 °C and 805 °C agree within a factor of 2 with previous tracer diffusion studies. However, below 700 °C in ferromagnetic α Fe-Ni, the $\tilde{D}$ values are up to two orders of magnitude smaller than previously determined by tracer diffusion.
4. The increase in diffusivity of ferromagnetic ternary α Fe-Ni-P over the diffusivity of ferromagnetic binary α Fe-Ni is related to the ratio of the amount of P in the diffusion couple to the amount of P soluble in α at the diffusion temperature.

ACKNOWLEDGMENTS

This research was supported by NSF through Grant EAR-8212531. We are grateful to Dr. R. Chou of Lehigh University who reviewed the manuscript.

REFERENCES

1. J.I. Goldstein, R.E. Hanneman, and R.E. Ogilvie: *Trans. TMS-AIME*, 1965, vol. 233, pp. 812-20.
2. C. Narayan and J.I. Goldstein: *Metall. Trans. A*, 1983, vol. 14A, pp. 2437-39.
3. T.R. Heyward and J.I. Goldstein: *Metall. Trans.*, 1973, vol. 4, pp. 2335-42.
4. C. Narayan and J.I. Goldstein: *Geochim. Cosmochim. Acta*, 1985, vol. 49, pp. 397-410.
5. A.D. Romig and J.I. Goldstein: *Metall. Trans. A*, 1980, vol. 11A, pp. 1151-59.
6. G. Cliff and G.W. Lorimer: *J. Micros.*, 1975, vol. 103, pp. 203-07.
7. J. Wood, D.B. Williams, and J.I. Goldstein: *J. Micros.*, 1984, vol. 255, pp. 255-75.
8. J.R. Michael: Ph.D. Dissertation, Lehigh University, Bethlehem, PA, 1984.
9. C. Wells and R.F. Mehl: *Trans. TMS-AIME*, 1941, vol. 143, pp. 329-39.
10. E.A. Balakir, Yu.P. Zotov, E.B. Malysheva, and V.I. Panchishnyy: *Aka. Nauk. SSR Izvestiia Metally*, 1974, vol. 5, pp. 198-200.
11. V. Ganessan, V. Seetharaman, and V.S. Raghunathan: *Mat. Letters*, 1984, vol. 2, no. 4A, pp. 257-62.
12. T. Ustad and H. Sorum: *Phys. Stat. Sol.(a)*, 1973, vol. 20, pp. 285-94.
13. K. Hoshino, Y. Iijima, and K. Hirano: *Acta Metall.*, 1982, vol. 30, pp. 265-71.
14. H.U. Helfmeier: *Z. Metallkde*, 1974, vol. 3, pp. 238-41.
15. A.D. LeClaire: *Phil. Mag.*, 1962, vol. 2, pp. 141-67.
16. A.D. LeClaire: *J. Nuclear Materials*, 1978, vol. 69, pp. 70-96.
17. A.S. Doan and J.I. Goldstein: *Metall. Trans.*, 1970, vol. 1, pp. 1759-67.
18. R.J. Borg and D.Y.F. Lai: *Acta Metall.*, 1963, vol. 11, pp. 861-66.
19. K. Hirano, M. Cohen, and B.L. Averbach: *Acta Metall.*, 1961, vol. 9, pp. 440-45.
20. Y. Chuang, Y.A. Chang, and R. Schmid: Paper No. 70, CALPHAD XIV, MIT, Cambridge, MA, June 9-14, 1985.
21. G.A. Bruggeman and J.A. Roberts: *Metall. Trans. A*, 1975, vol. 6A, pp. 755-60.
22. H. Hänsel, L. Stratmann, H. Keller, and H.J. Grabke: *Acta Metall.*, 1985, vol. 33, pp. 659-65.